SURFACE PASSIVATION APPLICABLE TO InAsSb/GaSb PHOTODIODES FOR INFRARED DETECTION

V. Odendaal[1], J.R. Botha[2] and F.D. Auret[3]

[1]*Denel Dynamics, P.O. Box 7412, Centurion, 0046, South Africa, Vicky.Odendaal@deneldynamics.co.za*
[2]*Department of Physics, Nelson Mandela Metropolitan University, P.O. Box 77000, Nelson Mandela Metropolitan University, Port Elizabeth 6031, South Africa, Reinhardt.Botha@nmmu.ac.za*
[3]*Department of Physics, University of Pretoria, Lynnwood road, Hillcrest, Pretoria, 0002, South Africa, fauret@postino.up.ac.za*

Abstract: In this paper the influence of various anodisation solutions on the surface passivation of InAsSb/GaSb photodiodes is examined. The diode structure is based on a design reported by Bubulac et al. [1]. The diode consists of a p-i-n structure grown by MOCVD and nearly lattice matched to a GaSb substrate. The structure, p-$InAs_{1-x}Sb_x$/n-$InAs_{1-x}Sb_x$/n-GaSb (x = 0.10 in both cases), consisted of a Zn-doped p-type layer and an unintentionally doped n-type layer on the n-type substrate. To define the active area of the photodiode, mesas were etched with a sulphuric acid based solution. Three anodisation solutions, containing Na_2S, KOH or $(NH_4)_2S$, were tested. Four sets of diodes were processed, using each of the three anodisation solutions as well as an unpassivated reference detector. The effect of passivation was studied by current-voltage measurements, yielding the reverse bias current, as well as by responsivity measurements.

Key words: Photodiode, surface passivation, anodisation, MOCVD, p-i-n structure, InAsSb.

1. INTRODUCTION

Given all the advantages offered by InAsSb several researchers have explored the possibilities of creating devices based on this compound. The greatest advantage of a ternary compound is the versatility that it allows one in engineering the size of the energy band gap. In the case of $InAs_{1-x}Sb_x$ the mole fraction of antimony in the compound can potentially vary the cut-off wavelength between 3.1 υm and 9.0 μm at 77 K, a spectral range hitherto dominated by the HgCdTe compound. InAsSb presents an improvement on some of the physical disadvantages given by HgCdTe. HgCdTe tends to be quite brittle, making handling and processing very difficult. This is caused by the large atomic numbers creating weak bonds with a large ionic component. The III-V family, to which the InAsSb compound belongs, possesses lower atomic numbers, causing stronger bonds of a more covalent nature. Another drawback of HgCdTe is that Hg diffuses at temperatures around 300 K. InAsSb can withstand processing steps at higher temperatures. From a material growth perspective the steep gradient of the HgCdTe band gap against Cd mole fraction relation presents a major challenge. The HgCdTe band gap has a much stronger dependence on the Cd mole fraction than the InAsSb band gap has on the Sb mole fraction. The practical implication is that the cut-off wavelength of detectors on a single HgCdTe wafer may differ from one surface area to the other - creating difficulties especially with detector matrix applications.

One of the greatest obstacles to overcome has been the lack of a suitable substrate for the production of high quality epitaxial layers. It is well-known that misfit dislocations, arising from lattice-mismatch between epitaxial structures and the substrate will cause defects, giving rise to trap assisted tunnelling, which in turn introduces a strong 1/f noise factor to the detector current [2] and severely limits the R_0A factor. The zero bias resistance of the detector, R_0, is the derivative of the I-V (current-versus-voltage) curve at zero bias voltage, this is influenced by both the material resistance and the size of the active area of the diode. The R_0A product, where A is the active area of the diode, is a figure of merit used to compare diodes with different active areas. Diodes with larger active areas tend to have smaller R_0 values.

Epitaxial growth of InAsSb on several substrates has been explored including GaSb [1, 3-6], GaAs [3, 7-11], and InAs [12-14]. Growth on GaAs or Si [15, 16] is a very attractive option because of the advantages it offers for the development of large area focal plane arrays and for the monolithic integration of the detector array with the readout circuit. Very high quality GaAs and Si substrates are readily available in large sizes. Even though Si technology is more established and extremely popular, it is possible to manufacture readout circuits on either Si or GaAs.

Rogalski et al. [17] explored the idea of growing $InAs_{1-x}Sb_x$ epitaxial layers on $Ga_{1-x}In_xSb$ substrates, which allows tuning of the lattice constant as well as the band gap of the substrate to complement that of the active layer.

Several workers have researched the qualities of InAsSb heterojunctions grown on GaSb substrates [3, 8, 10]. Srivastava et al. [3] have reported I-V and C-V measurements on n-$InAs_{0.95}Sb_{0.05}$/n-GaSb structures and found the n-n heterojunction to be strongly rectifying and behaving like a metal/n-GaSb Schottky diode with a barrier height of 0.8 ± 0.002 eV. They have established

that the band line up is of the broken gap variety. They have measured the valence band offset E_V(GaSb) - E_V(InAsSb) to be 0.67 ± 0.04 eV and concluded that the electrical characteristics of n-$InAs_{0.95}Sb_{0.05}$/n-GaSb heterojunctions are controlled by large band bending on the GaSb side of the junction.

Giani et al. [10] have done room temperature I-V measurements on lattice-matched n-$InAs_{0.91}Sb_{0.09}$/n-GaSb and p-$InAs_{0.91}Sb_{0.09}$/n-GaSb junctions. They also found the n/n heterostructure to be rectifying with a dark current of 70 μA at 1 V reverse bias. The p/n junction, on the other hand, was reported to be ohmic. This group measured the photoconductivity spectra of their n/n device at 300 K as well as at 77 K and found the response at 77 K to be nine times higher. They attributed this partly to an increase in the carrier lifetime.

Rakovska et al. [5] states that the GaSb/$InAs_{1-x}Sb_x$ interface is known to be semi-metallic, leading to massive flooding of the $InAs_{1-x}Sb_x$ layer by electrons from the valence band of the GaSb. In order to reduce the carrier population at the interface, they introduced a 30 nm $Al_{0.47}Ga_{0.53}Sb$ layer followed by an 18 nm $In_{0.85}Al_{0.15}As_{0.9}Sb_{0.1}$ layer to act as a barrier between the $InAs_{1-x}Sb_x$ layer and the GaSb. This resulted in narrower photoluminescence peaks and less noisy conductivity spectra.

Podlecki et al. [9] reported two types of noise behaviour for their MOCVD grown $InAs_{0.91}As_{0.09}$/GaAs diode structure. At low frequencies they observed a dominating 1/f noise that they attributed to non-optimised contacts. At higher frequencies they inferred noise due to generation-recombination processes.

In this paper the influence of the various surface passivation recipes tried in this study on the reverse bias dark current is examined for a photodiode based on a design reported by Bubulac et al. [1]. This group reported results on a p-i-n structure grown by LPE and nearly lattice matched to a GaSb substrate. The structure, p-$InAs_{1-x}Sb_x$ /n-$InAs_{1-x}Sb_x$/ n-GaSb (x = 0.10 in both cases), consisted of a Zn-doped p-type layer and an unintentionally doped n-type layer on the n-type substrate. In both cases the carrier density was reported to be 10^{16} cm^{-3}.

They observed a short wavelength cut on of 1.4 μm at 77 K, which is determined by the band gap of the GaSb substrate. The cut off wavelength was determined by the band gap of the n-InAsSb active region, which is composition dependent. They reported a 50 % cut off wavelength of 4 μm for devices with an antimony mole fraction of 0.10. AgMn was evaporated to establish ohmic contact to the front of the device and the backside contact was established by bonding the device with silver epoxy to a header; this also determined the aperture for backside illumination.

Bubulac et al. [1] determined the electron diffusion length to be almost 27 μm at 100 K and the hole diffusion length to be 5.5 μm. The hole diffusion length in GaSb was lower than in InAsSb. They established the GaSb reflection coefficient to be about 25 %. In their design they have placed the p-n junction 3 μm from the metallurgical interface with the substrate, i.e. less than the hole diffusion length, because shorter wavelength photons would be absorbed very close to the hetero-interface and holes would have to diffuse further to reach the junction. They measured the total InAsSb thickness to be 10 μm thick.

The photo-response of their detector covered a spectral range of 1.7 to 4.2 μm, achieving an external quantum efficiency of 65 % without anti-reflection coating. At 100 mV reverse bias, the diode current was measured to be less than 10^{-9} Acm^{-2}, with an R_0A product of 10^9 Ωcm^2.

2. EXPERIMENTAL METHODS

2.1 Device processing

The structure that was processed and evaluated in this work was based on the design by Bubulac et al. [1]. A p-i-n structure consisting of p-$InAs_{0.91}Sb_{0.09}$/n-$InAs_{0.91}Sb_{0.09}$/n-GaSb were grown by MOCVD, commissioned from Spire Bandwidth Semiconductor, LLC, situated in Hudson (New Hampshire, U.S.A). The (111)A GaSb substrate (487 μm thick) is Te doped to a carrier concentration of 2 x 10^{17} cm^{-3}. The p-$InAs_{0.91}Sb_{0.09}$ layer (7 μm thick) is Zn doped to a carrier concentration of 2 x 10^{18} cm^{-3} and the n-$InAs_{0.91}Sb_{0.09}$ layer (3 μm thick) not intentionally doped to a carrier concentration of 3 x 10^{16} cm^{-3}. The objective of this experiment was to investigate the effects of an anodic layer with respect to surface passivation. Previously [20] the success of the strategy was tested with the use of C-V measurements on MIS (Metal-Insulator-Semiconductor) devices. In this work the success of the passivation strategy will be evaluated through the resulting influence on the dark current and responsivity of an infrared photodetector.

A mesa pattern (diameter 4 mm)was first deposited by standard photolithographic procedures and etched to a depth of 8 μm. A sulphuric acid based etchant (H_2SO_4 (95-97 %) : H_2O_2 (30%) : H_2O, 50 ml : 1 ml : 100 ml) was used at 30 ˚C for 24 minutes, resulting in a mesa height varying from 7.5 μm to 8.8 μm. Next, an anodic layer was grown in order to passivate the etched surface. In addition to the three anodic solutions (KOH, Na_2S and $(NH_4)_2S$) one sample was left unpassivated to act as a reference. Finally a 6000 Å SiO_2 layer was deposited by UV enhanced CVD (ultraviolet enhanced chemical vapour deposition) to act as an anti-reflection layer before metal contacts were thermally evaporated. The metal contacts consisted of 60 nm Ti followed by 1.2 μm Au. In addition to achieving electrical contact, the metal layer

also served to define the front illuminated optical area with a 4 mm diameter.

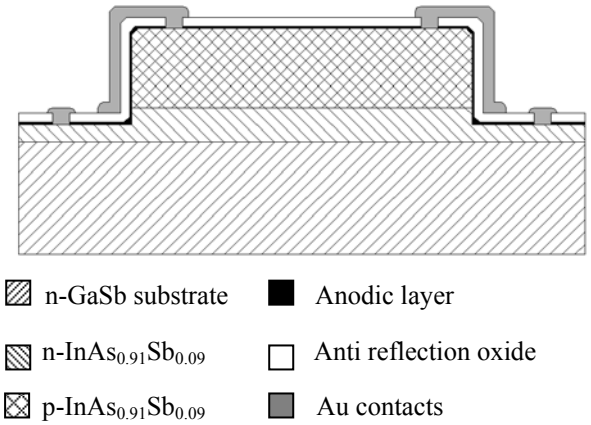

Figure 1: The InAsSb diode structure.

2.2 Current-versus-voltage measurements

All I-V measurements were done under dark room conditions. The I-V characteristics were measured using an Agilent 1500A parameter analyser. For room temperature measurements the I-V curve was measured from -1.5 V to +1.5 V with the current limited to 3 mA. For measurements at 77 K the output voltage was swept from -1 V to + 1 V with the current limited to 100 µA.

2.3 Electro-optical measurements

The relative responsivity was measured using a Nernst glow source. This source radiates a blackbody spectrum. By placing a monochromator in the optical path, specific wavelengths can be selected. The light from the monochromator was directed unto an optic table which reflected 30 % of the signal to a reference detector and 70 % to the processed InAsSb detector.

The reference detector was a ZnSe pyroelectric detector with a wavelength independent responsivity, in the range 1.2 µm to 14 µm. Due to the wavelength dependence of the monochromator throughput, the signal from the detector under test was normalised against the output from the reference detector.

In order to do absolute responsivity measurements, the diode structures were mounted inside experimental dewars, each with a sapphire window, yielding an average transmission of 80 % within the applicable wavelength region (i.e. 2.3 to 4.8 µm). The dewars were evacuated to a pressure below 2 x 10^{-2} mbar. The 20 % signal loss was compensated for in the calculations of the responsivity values.

The detector was set to view a 1000 K blackbody source. A chopper blade in the optical path modulated the signal at 2 kHz. The detector output was amplified by a low noise transimpedance amplifier with a gain of 1 MΩ and measured with an HP3561A dynamic signal analyser. To perform noise measurements the detector was positioned to view a blackbody at room temperature, with an emissivity of greater than 0.9.

3. EXPERIMENTAL RESULTS

Infrared photodiodes were processed on $InAs_{0.91}Sb_{0.09}$ as described in section 2.1. Four sets of diodes were processed, using each of the three anodisation procedures as well as an unpassivated reference detector. The relative responsivity measurements are shown in figure 2. Measurements were done on the untreated sample as well as the Na_2S treated sample, yielding identical results. The measured relative response results correspond very well to that of Remennyi et al. [14]. The detector spectral response yielded a short wavelength 50 % cut on at 3.3 µm and a long wavelength 50 % cut off at 4.3 µm.

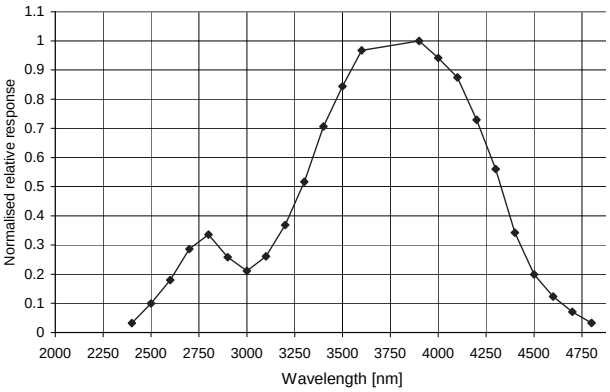

Figure 2: Measured relative response.

Current-versus-voltage (I-V) curves were measured on the four devices in order to investigate the influence of the various surface passivation techniques on the reverse bias dark current of the detectors.

The I-V curves measured on the $InAs_{0.91}Sb_{0.09}$ diodes, measured at room temperature in darkroom conditions, are displayed in figure 3. It can be seen that at room temperature the devices are rectifying.

The turn-on voltage (forward bias) of the diode is shown to be very sensitive to the anodizing solution used. This could be the quality of the anodization layer influencing the surface resistance and thus having an effect on surface leakage currents.

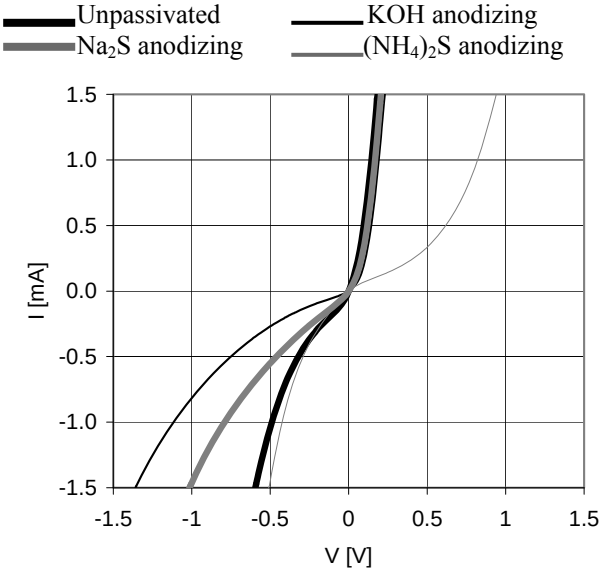

Figure 3: Current vs. voltage characteristics measured at 300 K.

Specific parameters extracted from the I-V curves measured at room temperature for the various surface passivation treatments, are presented in table 1. The parameters measured on a device that had no surface passivation treatment are shown as a reference. It is evident that at room temperature the best zero bias resistance (1270 Ω) was achieved for the sample anodised in KOH. For this device, the lowest zero and reverse bias dark current values are also obtained. Up to a reverse bias of 190 mV all three anodisation treatments seem to reduce the dark current values. For larger reverse bias voltages the $(NH_4)_2S$ passivation yields a dark current slightly larger than that of the reference sample.

Table 1: Device parameters extracted from current vs. voltage measurements at 300 K. Detector current measured at zero bias voltage, I_0, the detector current measured at 0.20 V, $I_{-0.200mV}$ and the detector current measured at 0.40V reverse bias voltage, $I_{-0.400mV}$, are shown.

Passivation	R_{series} [Ω]	R_{0V} [Ω]	I_{0V} [nA]	I_{-200mV} [μA]	I_{-400mV} [μA]
None	72	350	115.0	292.0	694.0
KOH anodising	74	1270	42.1	92.3	199.0
Na_2S anodising	98	824	95.1	165.0	456.0
$(NH_4)_2S$ anodising	202	1000	55.9	297.0	882.0

The dark I-V curves measured on the $InAs_{0.91}Sb_{0.09}$ diodes at 77 K, are shown in figure 4. Again rectifying behaviour is observed and the reverse bias dark current of the detectors are significantly smaller than at room temperature, due to a reduction in thermally generated carriers.

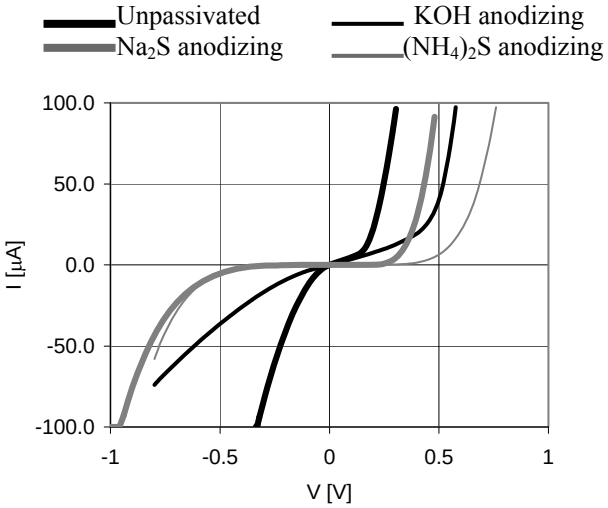

Figure 4: Current vs. voltage characteristics measured at 77 K.

Specific parameters extracted from the I-V curves measured at 77 K, after various surface passivation treatments, are summarised in table 2. At 77 K the highest zero bias resistance (28.5 MΩ) and the lowest zero bias current (4.7 pA) are achieved for $(NH_4)_2S$ passivation. Only for a reverse bias larger than 500 mV does the Na_2S surface passivation yield a lower detector current. All three anodisation treatments result in reduced dark currents as well as lower differential resistance.

Table 2: Device parameters extracted from current vs. voltage measurements at 77 K. Detector current measured at zero bias voltage, I_0, the detector current measured at 0.20 V, $I_{-0.200mV}$ and the detector current measured at 0.40V reverse bias voltage, $I_{-0.400mV}$, are shown.

Passivation	R_{series} [Ω]	R_{0V} [MΩ]	I_{0V} [nA]	I_{-200mV} [μA]	I_{-400mV} [μA]
None	115	0.02	10.7	40.8	100.0
KOH anodising	148	0.3	3.2	9.2	25.9
Na_2S anodising	134	18.4	0.08	0.1	1.9
$(NH_4)_2S$ anodising	379	28.5	0.005	0.1	1.9

Responsivity, noise and detectivity measurements were performed in order to investigate the influence of the various surface passivation treatments on the electro-optical performance of the devices.

The electro-optical parameters measured at 300 K are summarised in table 3. Performance parameters are compared as a result of the various surface passivation treatments. At room temperature the highest D*

(detectivity) is observed for the Na_2S anodisation (1.0 x 10^9 $cm^2Hz^{0.5}W^{-1}$). For this sample, the lowest noise was also achieved (3.9 x 10^{-12} $AHz^{-0.5}$). The unpassivated sample has the worst noise current and the lowest R_0A value.

Table 3: Influence of surface passivation on the electro-optical performance of the photodiode. Measurements were performed at 300 K.

Passivation	R_0A [Ω cm^2]	I_{noise} [pA $Hz^{-0.5}$]	R [mA/W]	D^*_{BB} [$cm^2Hz^{0.5}W^{-1}$]
None	44	6.3	12.0	7.6 x 10^8
KOH anodising	160	4.8	2.1	1.8 x 10^8
Na_2S anodising	104	3.9	10.0	1.0 x 10^9
$(NH_4)_2S$ anodising	126	5.9	7.1	4.4 x 10^8

The electro-optical parameters measured at 77 K are summarised in table 4. The sample passivated in Na_2S yielded the highest D* value at 1.1 x 10^9 $cm^2Hz^{0.5}W^{-1}$, with a noise current value of 3.7 x 10^{-13} $AHz^{-0.5}$. The lowest noise current (2.4 x 10^{-13} $AHz^{-0.5}$) and the highest R_0A value (3.6 x 10^6 Ωcm^2) were measured for the $(NH_4)_2S$ anodisation. All three anodisation treatments seem to improve the noise current by a factor of ~4 compared to that of the reference sample.

Table 4: Influence of surface passivation on the electro-optical performance of the photodiode. Measurements were performed at 77 K.

Passivation	R_0A [kΩ cm^2]	I_{noise} [pA $Hz^{-0.5}$]	R [mA/W]	D^*_{BB} [$cm^2Hz^{0.5}W^{-1}$]
None	2.3	1.1	2.7	9.6 x 10^8
KOH anodising	39.2	0.3	0.5	5.2 x 10^8
Na_2S anodising	2300	0.4	1.1	1.1 x 10^9
$(NH_4)_2S$ anodising	3600	0.2	0.4	7.7 x 10^8

The fact that the responsivity values are so low is ascribed to the quality of the material. The growth process is still being refined.

4. CONCLUSION

It is clear that the diode structure processed in this work displayed current rectification, resulting in a useful device in order to evaluate the success of the chosen surface passivation treatments. Current rectification was obtained at both room temperature as well as at 77 K.

All three anodisation solutions resulted in an improvement in the zero bias dark current over that of the reference diode structure. The highest 77 K D*-value (1.1 x 10^9 $cm^2Hz^{0.5}W^{-1}$) was achieved for the device anodised in Na_2S .

At 77 K the detector yielded a higher series resistance value, lower reverse bias dark current and higher differential resistance when compared to the values measured at room temperature. The noise current of the anodised samples was reduced by about an order of magnitude. The D* values of the KOH and $(NH_4)_2S$ anodised samples improved by about a factor of 2, while there was very little change in that of the untreated sample and the sample anodised in Na_2S. The noise current of the untreated sample improved only by a factor of 6 when cooled down to 77 K. At room temperature the detectors yielded higher current response values but also higher noise values, thus effectively eliminating the change in detectivity.

The highest detectivity value and the lowest noise current were achieved for the sample that had been treated in Na_2S. Thus Na_2S seems to be most effective in reducing the surface state density, which agrees with the results obtained from C-V measurements previously reported [18].

5. REFERENCES

[1] L. O. Bubulac, A. M. Andrews, E. R. Gertner, and D. T. Cheung: "Backside-illuminated InAsSb/GaSb broadband detectors", Appl. Phys. Lett. 36, pp. 734-736, 1980.

[2] A. Krier, H. H. Gao, and Y. Mao: "A room temperature photovoltaic detector for the mid-infrared (1.8-3.4 μm) wavelength region", Semicond. Sci. Tech. 13, pp. 950-956, 1998.

[3] K. Srivastava, J. L. Zyskind, R. M. Lurm, B. V. Dutt, and J. K. Klingert: "Electrical characteristics of InAsSb/GaSb heterojunctions", Appl. Phys. Lett. 49, pp. 41-43, 1986.

[4] A. Marciniak, R. L. Hengehold, Y. K. Yeo, and G. W. Turner: " Optical characterisation of molecular beam epitaxially grown InAsSb nearly lattice matched to GaSb", J. Appl. Phys. 84, pp. 480-488, 1998.

[5] A. Rakovska, V. Berger, X. Marcadet, B. Vinter, K. Bouzehouane, and D. Kaplan: "Optical characterization and room temperature lifetime measurements of high quality MBE-grown InAsSb on GaSb", Semicond. Sci. Technol. 15, pp. 34-39, 2000.

[6] Y. Mao, and A. Krier: "Liquid phase epitaxial growth and photoluminescence of InAsSb grown on GaSb substrates from antimony solution", J. Cryst. Growth 133, pp. 108-116, 1993.

[7] C. Besikci, S. Ozer, C. van Hoof, L. Zimmermann, J. John, and P. Mercken: " Characteristics of

$InAs_{0.8}Sb_{0.2}$ photodetectors on GaAs substrates ", Semicond. Sci. Tech. 16, pp. 992-996, 2001.

[8] G. Bethea, M. Y. Yen, B. F. Levine, K. K. Choi, and Y. Cho: "Long wavelength $InAs_{1-x}Sb_x$/GaAs detectors prepared by molecular beam epitaxy", Appl. Phys. Lett. 51, pp. 1431-1432. 1987.

[9] J. Podlecki, L. Gouskov, F. Pascal, F. Pascal-Delanoy, and A. Giani: "Photodetection at 3.65 μm in the atmospheric window using $InAs_{0.91}Sb_{0.09}$/GaAs heteroepitaxy", Semicond. Sci. Techn. 11, pp. 1127-1130, 1996.

[10] A. Giani, J. Podlecki, F. Pascal-Delannoy, G. Bougnot, L. Gouskov, and C. Catinaud: "Elaboration and characterization of InAsSb grown on GaSb and GaAs substrates", J. Cryst. Growth 148, pp. 25-30, 1995.

[11] A. Bansal, V. K. Dixit, V. Venkataraman, and H. L. Bhat: "Transport, optical and magnetotransport properties of hetero-epitaxial $InAs_xSb_{1-x}$/GaAs(x<=0.06) and bulk InAsxSb1-x(x<=0.05) crystals: experiment and theoretical analysis", Physica E 20, pp. 272-277, 2004.

[12] A. Krier, X. L. Huang, P. Fenge: "Fabrication and characterization of an $InAs_{0.96}Sb_{0.04}$ photodetector for MIR applications ", IEEE Electr. Device L. 25, pp. 283-285, 2004.

[13] P. Chakrabarti, A. Krier, X. L. Huang, P. Fenge, and R. K. Lal: "Optical and electrical characterisation of an p^+-$InAs_{0.96}Sb_{0.04}$/n^0-$InAs_{0.96}Sb_{0.04}$/n^+-InAs photodetector for mid-infrared application", Microwave and Optoelectronics Conference, 2003. IMOC 2003. Proceedings of the 2003 SBMO/IEEE MTT-S International, pp. 87-92 , 2003.

[14] M. A. Remennyi, N. V. Zotova, S. A. Karandashev, B. A. Matveev, N. M. Stus, and G. N. Talalakin: "Low voltage episide down bonded mid-IR diode optopairs for gas sensing in the 3.3–4.3 μm spectral range", Sensors and actuators B 91, pp. 256-261, 2003.

[15] W. Dobbelaere, J. de Boeck, M. van Hove, K. Deneffe, W. de Readt, R. Mertens, and G. Borghs: "Long wavelength $InAs_{0.2}Sb_{0.8}$ detectors grown on patterned Si substrates by molecular beam epitaxy", Electronics Letters, 26, pp. 259-261, 1990.

[16] T. Niedziela, and R. Ciupa: "Ultimate parameters of $Hg_{1-x}Cd_xTe$ and $InAs_{1-x}Sb_x$ n^+–p photodiodes", Solid State Electro. 45, pp. 41-46, 2001.

[17] A. Rogalski, R. Ciupa, and W. Larkowski: "Near room-temperature InAsSb photodiodes: Theoretical predictions and experimental data", Solid State Electro. 39, pp. 1593-1600, 1996.

[18] V. Odendaal, F. D. Auret and J. R. Botha: "On the processing of InAs and InSb for photodiode applications", Physica Status Solidi (c) 5, pp. 580-582, 2008.